Food Chemistry 214 (2017) 169–175

Contents lists available at ScienceDirect

Food Chemistry

journal homepage: www.elsevier.com/locate/foodchem

Analytical Methods

One-step competitive lateral flow biosensor running on an independent quantification system for smart phones based in-situ detection of trace Hg(II) in tap water

Nan Cheng [a], Yuancong Xu [a], Kunlun Huang [a,b], Yuting Chen [b], Zhansen Yang [b], Yunbo Luo [a], Wentao Xu [a,b,*]

[a] Beijing Advanced Innovation Center for Food Nutrition and Human Health, College of Food Science & Nutritional Engineering, China Agricultural University, Beijing 100083, China
[b] Beijing Laboratory for Food Quality and Safety, College of Food Science and Nutritional Engineering, China Agricultural University, Beijing 100083, China

ARTICLE INFO

Article history:
Received 4 March 2016
Received in revised form 7 July 2016
Accepted 9 July 2016
Available online 11 July 2016

Keywords:
Competitive lateral flow biosensor
Independent quantification system
Smart phones
Trace Hg(II)
Water detection

ABSTRACT

In this study, a one-step lateral flow biosensor (LFB) has been developed, optimized and validated for quantitative detection of Hg(II) in water. In the measurement principle, just one T-rich ssDNA probe (TSP) for the specific binding process was successfully employed in the competitive LFB based methods. The concept of an independent quantification system was realized using a cresol red dot as an external standard, which effectively eliminates false negative results. Under optimized conditions, the limit of detection for Hg(II) was 4 nM; high selectivity towards Hg(II) and extraordinary device-to-device repeatability of the LFB were achieved. Furthermore, Hg(II) from tap water samples was analyzed, and the results were confirmed by ICP-MS. The interference from other components in the real samples could be neglected during the analysis. The approach provides a simple, sensitive, and practical tool for the detection of trace Hg(II) in tap water, showing great promise for in-situ applications.

1. Introduction

The water-soluble mercury ion, present in its divalent ionic form at trace concentration levels, is one of the most common and extremely dangerous forms of heavy metal pollution that can have bioaccumulation and toxic effects on human health (Sekowski, Malkas, Wei, et al., 1997). Exposure even at an extremely low concentration of Hg(II) can damage the nervous and the digestive systems, especially the brain and kidney (Fong, Siu, Lee, et al., 2007). Many countries and organizations have regulated the upper limit of Hg(II) in drinking water samples. For example, the World Health Organization (WHO) specified a maximum allowable level of no more than 6 ng mL^{-1} (30 nM) for Hg(II) in drinking water (World Health Organization, 2004); the United States Environmental Protection Agency (EPA) has mandated the acceptable limit for Hg(II) in drinking water to be 2 ng mL^{-1} (10 nM) (Environmental Protection Agency, 2001); the European Union's (EU's) drinking water standards and Chinese Ministry of Health both specified a maximum allowable level of no more than 1 ng mL^{-1} (5 nM) for Hg(II) (European Union, 1998; Ministry of Health, 2007). Thus, routine detection of trace amounts of Hg(II) is central to global public health. Presently, conventional monitoring of Hg(II) frequently requires expensive modern instrumentation, including cold vapor atomic absorption spectroscopy (CV-AAS) (Shah, Kazi, Baig, et al., 2012), cold vapor atomic fluorescence spectrometry (CV-AFS) (Camera, Maranhão, Oliveira, et al., 2015), and electrothermal vaporization-inductively coupled plasma mass spectrometry (ETV-ICP-MS) (Yi, Jiang, & Sahayam, 2012). Despite the high sensitivity and accuracy that can be achieved by these analytical techniques, they require bulky instrumentation, skilled personnel and time-consuming sample pretreatment processes, which limit their wide applications in daily measurements (Yang, Song, Wang, et al., 2015).

To overcome these drawbacks, a variety of elegant sensing systems based on the specific binding capacity between two thymine (T) residues to form a T-Hg(II)-T base pair have been reported for colorimetric, fluorescent, electrochemical, and electrochemiluminescent detection of Hg(II) (Guo, Chen, Wang, et al., 2015; Li, Li, Wang, et al., 2009; Liu, Huang, & Chang, 2009; Zhou, Li, Chen, et al., 2013). For example, Li et al. reported a hemin-G-quadruplex-based colorimetric sensor for the detection of Hg(II) in an aqueous solution and achieved a detection limit of approximately 100 nM (Li et al., 2009). Moreover, Liu et al. designed a thrombin-binding aptamer probe labeled with FAM as a donor fluorophore, and a quencher, for the detection of Hg(II), which

* Corresponding author at: Beijing Laboratory for Food Quality and Safety, College of Food Science and Nutritional Engineering, China Agricultural University, Beijing 100083, China.
E-mail address: xuwentao@cau.edu.cn (W. Xu).

http://dx.doi.org/10.1016/j.foodchem.2016.07.058
0308-8146/

improved the sensitivity to 5 nM (Liu et al., 2009). Recently, Guo et al. used a gamma-polyglutamic acid-graphene-luminol composite in an electrochemiluminescence biosensor for Hg(II) detection with the limit of detection of 0.005 nM (Guo et al., 2015). The use of sensors made significant contributions to highly sensitive and specific Hg(II) detection; nevertheless, these methods have either limitations with respect to simplicity, repeatability, practicability or the requirement of multistep operations, making in-situ applications challenging (López Marzo, Pons, Blake, et al., 2013). Therefore, a simple, rapid, stable, one-step and cost-effective sensor for practical in-situ monitoring of trace Hg(II) remains desirable.

The lateral flow biosensor (LFB), as one of the most successful and widely commercially used in-situ screening techniques, has attracted considerable attention on Hg(II) analysis in recent years due to being **ASSURED**, which is **a**ffordable, **s**ensitive, **s**pecific, **u**ser-friendly, **r**apid, **e**quipment free and **d**eliverable to end-users (Ge, Asiri, Du, et al., 2014; Hu, Wang, Wang, et al., 2014; Liana, Raguse, Gooding, et al., 2012; Parolo & Merkoçi, 2013). Previously, two types of LFBs based on T-Hg(II)-T base pairs have been reported, namely the "two-step LFB" and "one-step sandwich LFB" (see details in Table S1) (Chen, Zhou, & Wen, 2014; Guo, Duan, Yang, et al., 2012; Liu, Chen, Chen, et al., 2014; Yang, Duan, Li, et al., 2012; Zhu, Wang, Deng, et al., 2014). Two-step LFBs with super-sensitivity were usually based on well-designed DNA machines for signal amplification which triggered by Hg(II), but these methods were unable to achieve the signal amplification and detection steps at the same time, which would inhibit the application for in-situ detection in remote areas (Chen et al., 2014; Liu et al., 2014). One-step sandwich LFBs were more practical, however, using two T-rich ssDNA probes and Hg(II) to form the complicated sandwich structure in a short reaction time, though this could give false negative results that limited the spread and usage (Guo et al., 2012; Yang et al., 2012; Zhu et al., 2014). Nevertheless, there is still room for principle simplification or performance improvement of LFBs for trace Hg(II) detection.

Herein, for the first time, we report on the development of a competitive lateral flow nucleic acid biosensor running on an independent quantification system for smart phones for in-situ detection of trace Hg(II) in one-step. Just one T-rich ssDNA probe (TSP) was employed on the LFB for Hg(II) detection though the specific binding process and a practical sensitivity was achieved with this method under the optimized conditions. The proposed method not only effectively eliminates false negative results but also exhibits high selectivity towards Hg(II) and extraordinary device-to-device repeatability among the six replicate determinations. Furthermore, the practical applications of the LFB were verified by detecting spiked Hg(II) in tap water samples.

2. Materials and methods

2.1. Chemicals and materials

Chloroauric acid tetrahydrate ($HAuCl_4{\cdot}4H_2O$), trisodium citrate, sodium citrate dihydrate, Triton X-100, mycose, sodium dodecyl sulfonate (SDS), NaCl, $Na_3PO_4{\cdot}12H_2O$, Tween-20, sucrose, deoxyadenosine triphosphate (dATP), bovine serum albumin (BSA), phosphate buffered saline (PBS, pH 7.4, 0.01 M), sodium chloride–sodium citrate (SSC) buffer (20 concentrate, pH 7.0), borate buffer (BB, pH 9.0, 0.1 M) and the metal salts used in this study ($Hg(NO_3)_2$, $Zn(NO_3)_2$, $Mg(NO_3)_2$, $Pb(NO_3)_2$, $Fe(NO_3)_3$, $Fe(NO_3)_2$, $Cu(NO_3)_2$, KNO_3, $Ca(NO_3)_2$, $Mn(NO_3)_2$ and $Ni(NO_3)_2$) were purchased from Sigma Chemical Company (St. Louis, MO, USA). Streptavidin was purchased from Invitrogen (Carlsbad, CA, USA). Double distilled water (ddwater) was used in all experiments.

Backing cards (HF000MC100), glass fiber sample pads (CFSP001700), conjugation pads (GFCP000800), nitrocellulose membranes (135 s) and absorbent pads (CFSP001700) were purchased from Millipore (Bedford, MA, USA).

All DNA sequences were synthesized and purified by Sangon Biotech Co., Ltd. (Shanghai, China), and their sequences are shown in Table S2.

2.2. Synthesis of Au-NPs

Au-NPs were synthesized following a previous method with a little modification (Gao, Xu, Baloda, et al., 2014; Lie, Liu, Fang, et al., 2012). Briefly, a 50 mL aqueous solution of 2.4×10^{-4} M $HAuCl_4$ was heated to boiling, and then 1.67 mL of 1% trisodium citrate was added. The boiling solution was stirred for another 30 min, and then stored at 4 °C prior to use. TEM images showed the diameter of such Au-NPs ~20 nm, and the UV–vis spectrum exhibited a characteristic plasmon absorption band with a maximum at 520 nm (as shown in Figs. S1A and S1B).

2.3. Modification of Au-NPs by DNA probes

Au-NPs modified by DNA probes were prepared by a modified method according to the literature (Fang, Huang, Lie, et al., 2010; Gao et al., 2014). Procedures were as follows: 30 μL of 100 mM of dATP was added into 1 mL of concentrated Au-NP solution to protect Au-NPs from salt-induced aggregation. The mixture was incubated at room temperature for 20 min. 15 μL of 1% of SDS was slowly added into the mixture, and incubated on a shaker for 10 min. 20 μL of 1 M NaCl was dropped into the mixture at a rate of 5 μL/10 min. Then, 0.5 OD of each thiolated DNA probe which is required was added, and the mixture was incubated for 4 h in metal bath at 60 °C. After the incubation, the mixture was centrifuged at 12,000 rpm for 15 min, and the supernatant was discarded. Then, the deposited Au-NPs were washed with 1 mL of PBS and dispersed in 20 μL of storage buffer (containing 20 nM of $Na_3PO_4{\cdot}12H_2O$, 5% BSA, 0.25% Tween-20 and 10% sucrose). Figs. S2A and S2B show the TEM image and the UV–vis absorption spectra of Au-NPs modified by the DNA probes after centrifugation, respectively, from which the monodispersion of Au-NPs and the surface plasmon absorption of Au-NPs slightly shifted to 522 nm were observed.

2.4. Conjugation of streptavidin-biotinylated DNA

The streptavidin solution and probe solution were prepared by dissolving the appropriate amount of streptavidin and biotinylated DNA in solubilizing buffer (PBS containing 0.5% mycose). Briefly, 30 μL of 1 mg/ml of streptavidin solution was mixed with 30 μL of 100 μM DNA probe solution. The mixture was incubated at room temperature for 1 h and stored at 4 °C until use.

2.5. Preparation of LFB

The LFB consisted of the following five components: a sample pad, conjugate pad, nitrocellulose membrane, absorbent pad, and backing. The sample pad (17 mm × 30 cm) and conjugate pad (8 mm × 30 cm) were made from glass fiber and saturated with a buffer (pH 8.0) containing 0.25% Triton X-100, 0.1 M BB, and 0.15 M NaCl. Then, the pad was dried at 37 °C for 2 h and stored in a desiccator. A test line (1 μL/cm) and control line (1 μL/cm) were prepared by dispensing 30 μL of streptavidin-biotinylated DNA conjugates at different locations on the nitrocellulose membrane (25 mm × 30 cm) using a BioDot BioJet BJQ 3000 dispenser (Irvine, CA). The distance between each line was approximately 5 mm. The nitrocellulose membranes were then dried overnight

at 37 °C and stored at 4 °C. The different pads were assembled on backing (60 mm × 30 cm) with an overlap between them of approximately 1–2 mm to ensure that the solution could migrate through the biosensor. LFBs were cut at a width of 3 mm using a Bio-Dot Paper Cutter module CM4000 (Irvine, CA).

2.6. Detection of trace Hg(II)

In a typical test (see diagram in Fig. S3), 50 μL of running buffer (4 concentrate SSC containing 2% BSA and 0.05% Tween-20) with the desired amount of Hg(II) was applied to the sample pad. 2.5 μL of DNA probe modified Au-NP conjugates were loaded on the conjugate pad. During the assay process, the solution migrated up by capillary force. Then, the presence of Hg(II) in the samples was determined by visual observation within 5 min. For quantitative measurements, 1 μL of cresol red (5 ppb, pH 9.0) was added on the absorbent pad as an external standard, and the color intensity of the test line (Red-Green-Blue value, RGB) and the cresol red dot (R_m, G_m, B_m) were recorded using a color-analysis app (such as Color, Color Curous and Its Colors, etc.) which was preloaded on a smart phone. We recorded the RGB values ten times for each line: at the upper segment three times, the middle segment four times and the lower segment three times so that average figures would be available. In the independent quantification system, the relative intensity is defined as R/R_m. The smart phones with greater than or equal to 8-megapixel cameras had no significant effect on collecting color data ($P > 0.05$, see details in Table S3).

2.7. Detection of trace Hg(II) in tap water samples

Tap water samples were obtained from three communities (Code: A, B and C) in the southeastern Haidian District, Beijing, China. Spiked samples were prepared by adding Hg(II) at specific concentrations. Then, spiked and nonspiked samples were detected with the LFB as described above for three times. All detection results were further confirmed by the ICP-MS method (Allibone, Fatemian, & Walker, 1999).

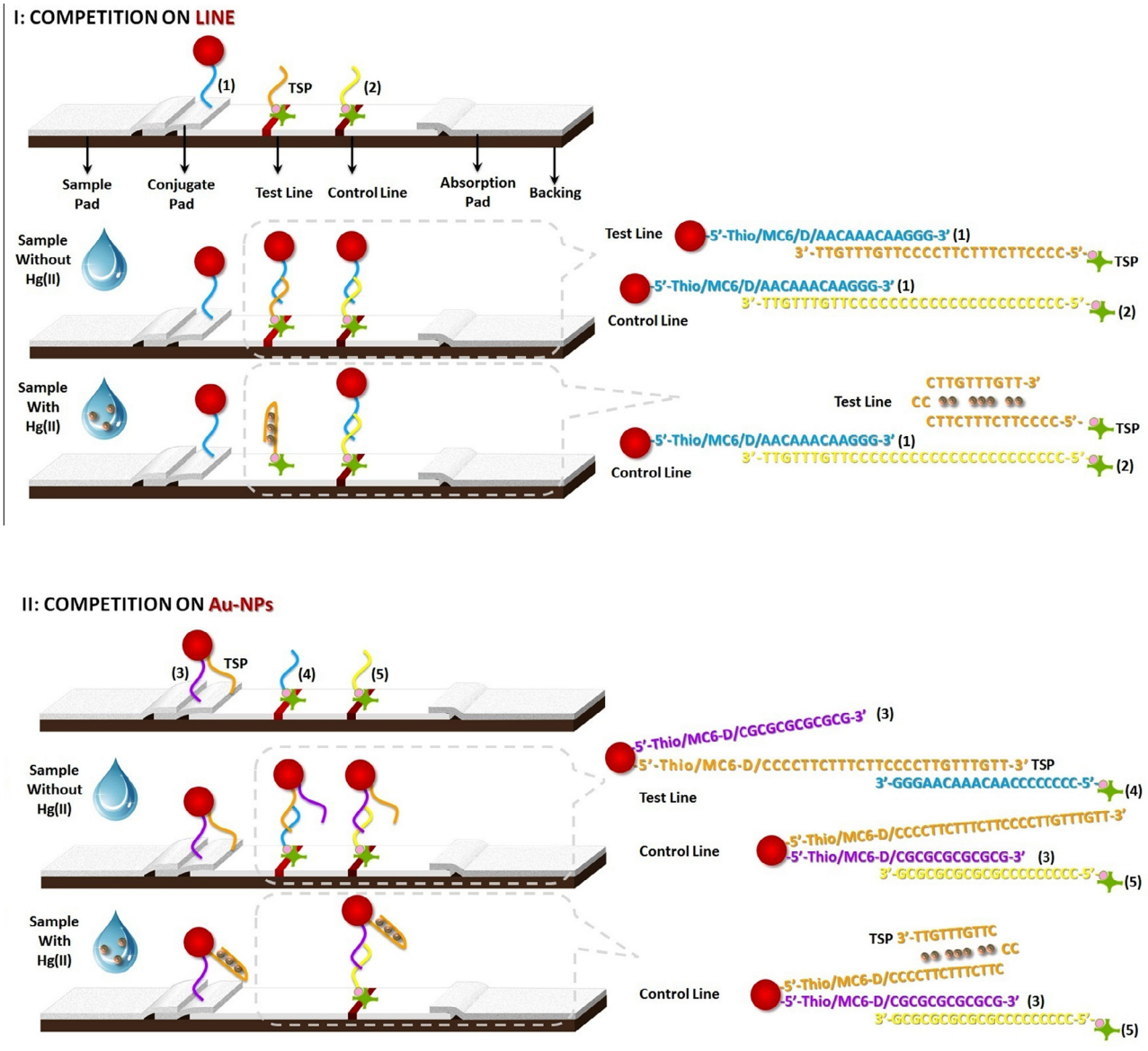

Scheme 1. Schematic of the design of the competitive LFB: (I) Competition on line; (II) Competition on Au-NPs.

3. Results and discussion

3.1. Principles of competitive LFB

We proposed two modes of immobilization of TSP for a competitive LFB to recognize trace Hg(II). In the first mode, named "competition on line" (Scheme 1A), the biotin-TSP is directly immobilized on the test line via a biotin-streptavidin interaction. Another biotin-DNA probe (2) was also linked with streptavidin and dispensed on the nitrocellulose membrane to form the control line. The thiolated-DNA probe (1) was immobilized on the Au-NPs, and the resulting Au-NPs-DNA probe (1) conjugate was loaded on the conjugate pad. Typically, the sample solution without Hg(II) is applied on the sample application pad. The solution migrates by capillary action and passes the conjugate pad. Then, the hybridization between the DNA probe (1) of conjugate and the immobilized TSP occurs on the test line. The accumulation of Au-NPs is visualized as a characteristic red band. The excess conjugates continue to migrate and are captured by the DNA probe (2), thus forming a second red band on the control line. In the presence of Hg(II), the competitive reaction happens between the DNA probe (1) and Hg(II) to combine with TSP. As a result, Hg(II) combines with TSP, decreasing the Au-NPs-DNA probe (1) conjugate that could hybridize to TSP, and causes the red color intensity to become weaker. In other words, the more Hg(II) in the samples, the weaker the intensity on the test line.

Another mode of competitive LFB, named "competition on Au-NPs" (Scheme 1B), is designed by using thiolated-TSP and a thiolated-DNA probe (3) immobilized on the Au-NPs via an Au-S bond which is loaded on the conjugate pad. Two DNA probes (4 and 5) were immobilized on the nitrocellulose membrane to form the test line and control line, respectively. In the absence of Hg(II), the hybridization between the TSP of conjugate and the immobilized DNA probe (4) occur on the test line, then a characteristic red band could be observed due to the accumulation of Au-NPs. Once the solution passed through the control zone, the excess conjugates were captured by the biotinylated DNA probe (5), and thus a second black band appeared. For a sample solution with Hg(II), the TSP of the conjugate combines with Hg(II) first on the conjugate pad, then decreases the hybridization between the TSP and DNA probe (4) on the test line. Similarly, the more Hg(II) in the samples, the weaker the intensity on the test line.

3.2. Optimization of competitive LFB

3.2.1. Selection between two principles

Considering that the accumulation of Au-NPs on the test line could affect the responses of the LFB, two competitive principles were investigated by comparing the performance of the test line with specific concentrations of Hg(II) in the samples. Fig. 1A presents a universal result judgment method, and Fig. 1B shows the typical images of the LFBs following the two principles for a test with 0, 64 and 2048 nM of Hg(II). The first principle, named "competition on line", presented a greater ability to weaken the accumulation of Au-NPs on the test at 64 nM of Hg(II) than the second principle named "competition on Au-NPs" because there is an excess of the Au-NPs-DNA probe conjugates loaded on the conjugate pad to ensure the two lines appear without Hg(II) in the samples. However, when trace amounts of Hg(II) showed up, excess Au-NPs-DNA probe conjugates still hybridized the probe on the test line under the second principle, while this phenomenon did not exist in the first principle. Therefore, the first principle named "competition on line" was selected in the following experiments.

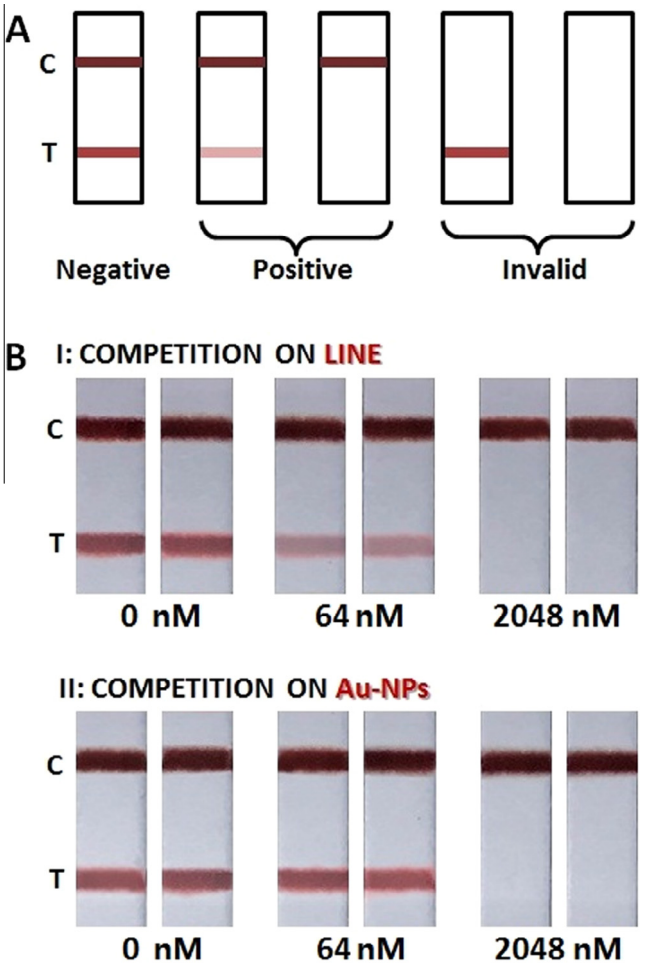

Fig. 1. (A) The universal result judgment method of proposed LFBs. (B) Typical images of LFBs following the two competitive principles for 0, 64 and 2048 nM of Hg(II) test: (I) Competition on line; (II) Competition on Au-NPs. The images were recorded with a camera phone (12-megapixel).

3.2.2. Key factors of LFB determination

After development of the competitive LFB principle, many key factors of LFBs should be optimized to minimize the nonspecific adsorption and simultaneously maximize the sensitivity and reproducibility. First, the volume of Au-NPs-DNA probe conjugates significantly influenced the intensity of the lines. The color results from increasing volumes of the Au-NPs-DNA probe conjugates loaded on the conjugate pad, ranging from 0.5 μL to 2.5 μL, were compared and 2.0 μL of Au-NPs-DNA probe conjugates was found to be the optimal volume for detection (see details in Fig. S4). The length of C-rich linker DNA in TSP and the length of C-rich scaffold DNA on the control line are also of importance to the performance of LFBs. The optimal length of the C-rich linker DNA in TSP was four bases, and the length of C-rich scaffold DNA on the control line was found to be 19 bases (see details in Table S4). A proper external standard solution for quantitative determination, containing 1 μL of cresol red (5 ppb, pH 9.0), was also optimized (see details in Fig. S5). A suitable running buffer, containing 4 × SSC, 2% BSA and 0.05% Tween-20, provided the optimum combination for clear bands, rapid tests, and background elimination and was used throughout the entire study (see details in Fig. S6).

3.3. Sensitivity of competitive LFB

Under optimal experimental conditions, the sensitivity of the LFB was tested with ddwater spiked with Hg(II) at concentrations

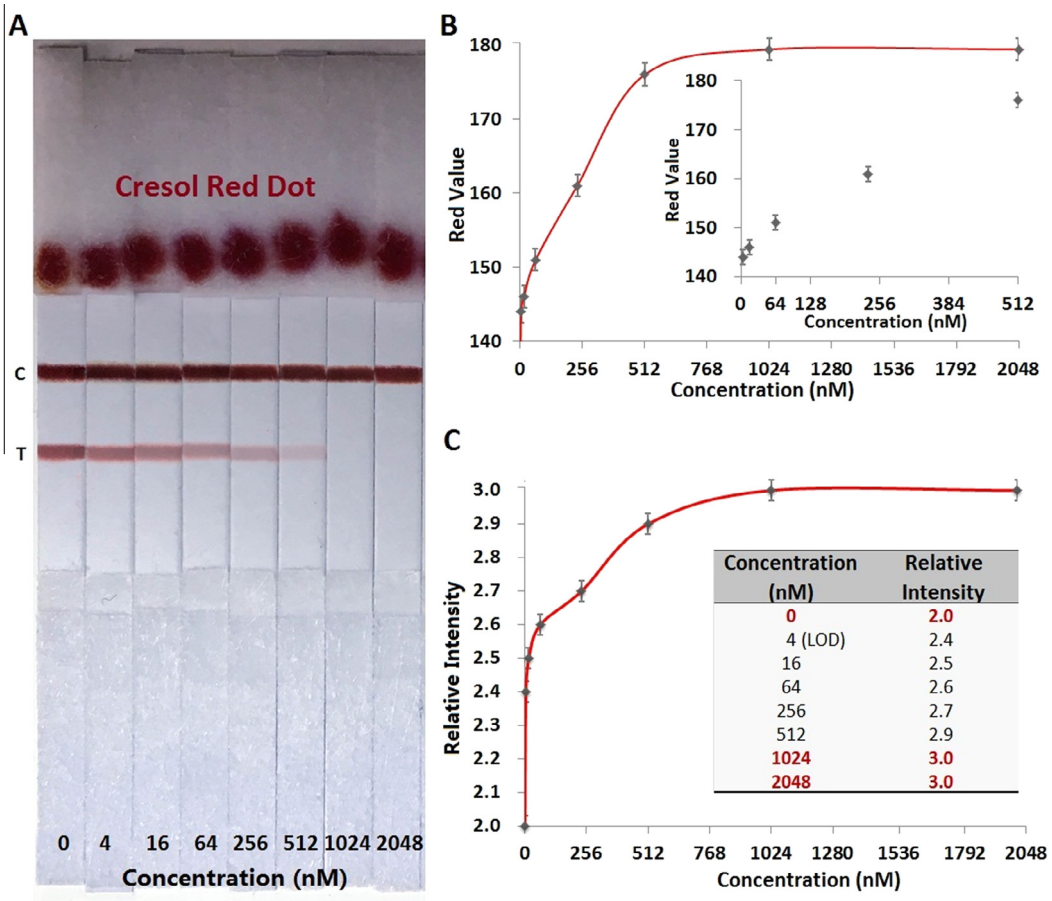

Fig. 2. (A) Photo images of LFBs in response to various concentrations of Hg(II). The images were recorded with a camera phone (12-megapixel). (B) The inhibition curve of the LFB with different concentrations of Hg(II). The corresponding color intensities were recorded with a color-analysis app named Color. (C) Relative intensity curve of the LFB with different concentrations of Hg(II). A checklist was inserted to promote the ability of LFB to find and analyze quickly. Each point represents the mean of thirty measurements from triplicate separate experiments. The 95% confidence interval for each mean is between the error bars.

of 0–2048 nM. Fig. 2A shows the typical images of LFBs in response to various concentrations of Hg(II). The color intensity of the test line decreased with increasing concentrations of Hg(II) in the standard samples. False positive results and false negative results were not obtained in any of the tests. As shown in Fig. 2B, the red values are linearly dependent on the concentration of Hg(II) in the ranges 4 nM-64 nM and 64 nM-512 nM. The correlation equations are Red Value = 143.83 + 0.1131$c_{Hg(II)}$ (nM) [correlation coefficient: R^2 = 0.9918] and Red Value = 147.62 + 0.0556$c_{Hg(II)}$ (nM) [correlation coefficient: R^2 = 0.9996], respectively. Thus, the assay is a field-portable, cost-effective, and smart phone based platform to sensitively quantify Hg(II) concentration in tap water samples. Similarly, the data of the Green and Blue values point toward the same trend (data not shown). The limit of detection (LOD) of the LFB was quantitatively defined here as the amount of Hg(II) in the standard sample solution that caused relative intensity of greater than 2. In the present study, the LOD was 4 nM as shown in Fig. 2C, which satisfactorily meets the drinking water requirement of the above mentioned countries and multinational organizations.

3.4. Interference of potential metal ions

To study the selectivity of the competitive LFB, a series of metal ions including Zn(II), Mg(II), Pb(II), Fe(III), Fe(II), Cu(II), K(I), Ca(II), Mn(II) and Ni(II), each with a concentration of 2048 nM were tested. As shown in Fig. 3, only 4 nM of Hg(II) showed detectable lower color intensity on the test line and 2048 nM of Hg(II) showed significantly low color intensity on the test line, while the LFB hardly detects debilitated signals to other metal ions and blank. These results demonstrate an excellent selectivity of the proposed assay for Hg(II) analysis against other environmentally relevant potential metal ions, which is attributed to the highly specific coordination of mismatched base pair. This test indicates the developed competitive LFB has a good selectivity for Hg(II) ions.

3.5. Reproducibility and stability of competitive LFB

The signal reproducibility was one of the most important criteria in evaluating the sensing system. The device-to-device reproducibility of the proposed competitive LFB was evaluated by analyzing one sample for six replicate determinations. Sample solutions containing 0, 64 and 2048 nM Hg(II) were used to examine the performance of the LFB (see data in Table S5). As shown in Fig. 4, similar responses could be obtained against each concentration. The corresponding RSD values of the optical responses for 0, 64 and 2048 nM were 1.7%, 1.9% and 2.6%, respectively, indicating the excellent device-to-device reproducibility of the measurements.

The shelf life of the strip device was examined during a one year period using the same batch of strips. Strips were stored in Ziploc bags under dark and dry conditions at 20° to 25 °C and intermittently measured (every 10 days) the same concentration of Hg (II). During the stability examination, the intensity of the red bands

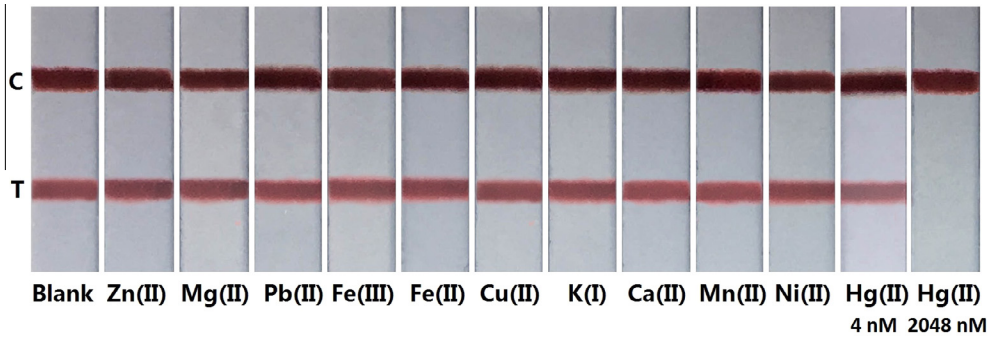

Fig. 3. Selectivity of the LFB for Hg(II) over other potential metal ions. The concentration of the other metal ion is 2048 nM. The concentrations of Hg(II) are 4 nM and 2048 nM. The images were recorded with a camera phone (12-megapixel).

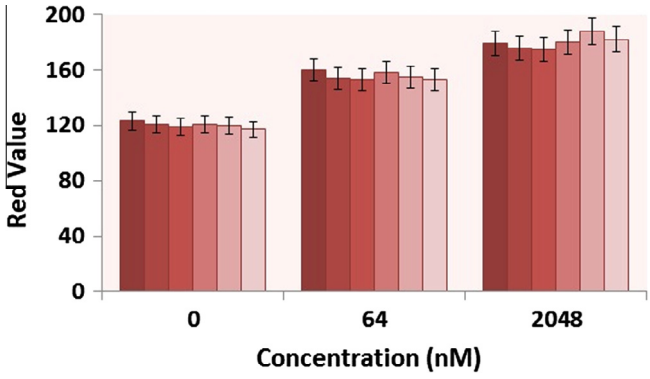

Fig. 4. Device-to-device reproducibility of the LFB for Hg(II) detection. Hg(II) concentration: 0, 64, 2048 nM; RSD: 1.7%, 1.9%, 2.6%; n = 6.

on the lines performed over 3 months was exactly the same as that in the first day. The intensity of the red bands at 12 months was less than 5% compared to those in the first day (data not shown), which showed no significant loss for Hg(II) detection. Thus, the strip device was still usable after 12 months storage, indicating that the competitive LFB approach is very promising with respect to applications for the in-situ detection of Hg(II).

3.6. Application of competitive LFB

To further test the feasibility in practical use, the introduced competitive LFB had been applied to assay Hg(II) in real tap water samples. The samples spiked with different concentrations of Hg (II) were detected according to the general procedure. The results are summarized in Table 1. All of the recoveries were between 93 and 107%, which indicated that the interference of materials in tap water, such as bacteria and disinfectant, did not interact with the LFB. Moreover, the data revealed that no significant difference existed between the values measured using the proposed LFB and ICP-MS, confirming the accuracy of the developed strip for detecting Hg(II). The above results demonstrate that such a device can be applied in the analysis of real samples. By this method, the water samples can be easily examined to see whether they have been contaminated by trace Hg(II).

4. Conclusions

In summary, we have developed a simple and one-step competitive LFB for a smart phone based in-situ detection method of trace Hg(II) in tap water. Such an LFB possesses four unusual superiorities: 1) **One-step operation.** Compared with conventional

Table 1
Determination of Hg(II) in tap water samples using the LFB and ICP-MS.

Tap water sample	Spiked Hg (II) (nM)	LFB[a] (nM)	Recovery (%)	ICP-MS[b] (nM)	Relative error[c] (%)
No. 1[e]	0	Negative		ND[d]	
	4	4.2 ± 1.9	105	3.9 ± 0.6	7.7
No. 2[f]	0	Negative		ND	
	16	17.1 ± 2.3	107	15.7 ± 0.8	9.0
No. 3[g]	0	Negative		ND	
	64	59.7 ± 4.1	93	62.3 ± 2.3	−4.2
No. 4[g]	0	Negative		ND	
	256	247.3 ± 5.7	97	251.6 ± 2.9	−1.7
No. 5[g]	0	Negative		ND	
	512	491.0 ± 6.4	96	502.8 ± 3.1	−2.3

[a] Each sample was analyzed using our proposed LFBs, and all values were obtained as an average of three repetitive determinations ± standard deviation (mean ± SD).
[b] The concentration of Hg(II) in water samples was certified using ICP-MS.
[c] LFB vs ICP-MS method.
[d] Not Detected.
[e] The tap water sample was obtained from communitiy A.
[f] The tap water sample was obtained from communitiy B.
[g] The tap water sample was obtained from communitiy C.

methods and previous elegant sensing systems, the current one-step LFB approach with much respect to simplicity, repeatability and practicability can avoid the use of specialized instruments and the requirement of highly qualified personnel. After systematic optimization, the LFB was able to detect a minimum concentration of 4 nM Hg(II), which was suitable for quantitative work. 2) **Competitive principle design.** For the first time, just one TSP for the specific binding process, which can eliminate the complex structures on test line, was successfully employed in the competitive principle design on the basis of T-Hg(II)-T base pair. Moreover, the design can expand the application for other metal ions, such as Cu(II), Ni(II) and Co(II), which can bind with specific nucleotide bases to form metal-ion-mediated base pairs (Clever, Kaul, & Carell, 2007; Tanaka, Oda, Yamaguchi, et al., 2007; Zhang, Lin, Yang, et al., 2012), to build multilevel LFBs. 3) **Smart phone based in-situ detection.** We demonstrated the first application of camera phone based in-situ detection method by recording RGB values of the LFB, which can be implemented using a color-analysis app preloaded in a smart phone with potential practical significance. 4) **Independent quantification system.** The most notable feature of the LFB developed in this effort is their intelligent and practical design for an independent quantification system using a cresol red dot as the external standard, which can effectively eliminate false negative results above the LOD (4 nM). In contrast to previous competitive LFB work, the determination with no need for comparison with blank sample is more useful and convenient, which

revealed excellent performance and is capable of detecting Hg(II) in real samples, illuminating the potential application of the design. With these advantages, our work not only provides a one-step and competitive assay for Hg(II) detection but also presents a new class of LFBs with independent quantification system for smart phone based in-situ monitoring of tap water.

Acknowledgment

This work was supported by the Ministry of Science and Technology of Beijing (XX2014B069).

Appendix A. Supplementary data

Supplementary data associated with this article can be found, in the online version, at http://dx.doi.org/10.1016/j.foodchem.2016.07.058.

References

Allibone, J., Fatemian, E., & Walker, P. J. (1999). Determination of mercury in potable water by ICP-MS using gold as a stabilising agent. *Journal of Analytical Atomic Spectrometry, 14*(2), 235–239.

Camera, A. S., Maranhão, T. A., Oliveira, F. J. S., et al. (2015). Total mercury determination in petroleum green coke and oily sludge samples by cold vapor atomic fluorescence spectrometry. *Journal of the Brazilian Chemical Society, 26*(10), 2116–2124.

Chen, J., Zhou, S., & Wen, J. (2014). Disposable strip biosensor for visual detection of Hg^{2+} based on Hg^{2+}-triggered toehold binding and exonuclease III-assisted signal amplification. *Analytical Chemistry, 86*(6), 3108–3114.

Clever, G. H., Kaul, C., & Carell, T. (2007). DNA–metal base pairs. *Angewandte Chemie International Edition, 46*(33), 6226–6236.

Drinking Water Health Standards (2007). *GB5749-2006*. China: Ministry of Health.

European Union's drinking water standards. (1998). Council Directive 98/83/EC on the quality of water intented for human consumption. Adopted by the Council, on 3 November.

Fang, Z., Huang, J., Lie, P., et al. (2010). Lateral flow nucleic acid biosensor for Cu2+ detection in aqueous solution with high sensitivity and selectivity. *Chemical Communications, 46*(47), 9043–9045.

Fong, B. M. W., Siu, T. S., Lee, J. S. K., et al. (2007). Determination of mercury in whole blood and urine by inductively coupled plasma mass spectrometry. *Journal of Analytical Toxicology, 31*(5), 281–287.

Gao, X., Xu, H., Baloda, M., et al. (2014). Visual detection of microRNA with lateral flow nucleic acid biosensor. *Biosensors and Bioelectronics, 54*, 578–584.

Ge, X., Asiri, A. M., Du, D., et al. (2014). Nanomaterial-enhanced paper-based biosensors. *TrAC Trends in Analytical Chemistry, 58*, 31–39.

Guo, Z., Chen, B., Wang, Z., et al. (2015). An electrochemiluminescence biosensor for mercury ion detection based on gamma-polyglutamic acid-graphene-luminol composite and oligonucleotides. *Sensors and Actuators B: Chemical, 209*, 579–585.

Guo, Z., Duan, J., Yang, F., et al. (2012). A test strip platform based on DNA-functionalized gold nanoparticles for on-site detection of mercury (II) ions. *Talanta, 93*, 49–54.

Hu, J., Wang, S. Q., Wang, L., et al. (2014). Advances in paper-based point-of-care diagnostics. *Biosensors and Bioelectronics, 54*, 585–597.

Li, T., Li, B., Wang, E., et al. (2009). G-quadruplex-based DNAzyme for sensitive mercury detection with the naked eye. *Chemical Communications, 24*, 3551–3553.

Liana, D. D., Raguse, B., Gooding, J. J., et al. (2012). Recent advances in paper-based sensors. *Sensors, 12*(9), 11505–11526.

Lie, P., Liu, J., Fang, Z., et al. (2012). A lateral flow biosensor for detection of nucleic acids with high sensitivity and selectivity. *Chemical Communications, 48*(2), 236–238.

Liu, J., Chen, L., Chen, J., et al. (2014). An autonomous T-rich DNA machine based lateral flow biosensor for amplified visual detection of mercury ions. *Analytical Methods, 6*(7), 2024–2027.

Liu, C. W., Huang, C. C., & Chang, H. T. (2009). Highly selective DNA-based sensor for lead (II) and mercury (II) ions. *Analytical chemistry, 81*(6), 2383–2387.

López Marzo, A. M, Pons, J., Blake, D. A., et al. (2013). High sensitive gold-nanoparticle based lateral flow Immunodevice for Cd2+ detection in drinking waters. *Biosensors and Bioelectronics, 47*, 190–198.

Parolo, C., & Merkoçi, A. (2013). Paper-based nanobiosensors for diagnostics. *Chemical Society Reviews, 42*(2), 450–457.

Sekowski, J. W., Malkas, L. H., Wei, Y., et al. (1997). Mercuric ion inhibits the activity and fidelity of the human cell DNA synthesome. *Toxicology and Applied Pharmacology, 145*(2), 268–276.

Shah, A. Q., Kazi, T. G., Baig, J. A., et al. (2012). Simultaneously determination of methyl and inorganic mercury in fish species by cold vapour generation atomic absorption spectrometry. *Food Chemistry, 134*(4), 2345–2349.

Tanaka, Y., Oda, S., Yamaguchi, H., et al. (2007). 15N–15N J-coupling across HgII: Direct observation of HgII-mediated TT base pairs in a DNA duplex. *Journal of the American Chemical Society, 129*(2), 244–245.

United States Environmental Protection Agency (2001). *Mercury update impact on fish advisories, EPA fact sheet EPA-823-F-01-011*. Washington, DC: Office of Water.

World Health Organization (2004). *Guidelines for drinking-water quality: Recommendations*.

Yang, F., Duan, J., Li, M., et al. (2012). Visual and on-site detection of mercury (II) ions on lateral flow strips using DNA-functionalized gold nanoparticles. *Analytical Sciences, 28*(4), 333.

Yang, R., Song, D., Wang, C., et al. (2015). Etching of unmodified Au@ Ag nanorods: A tunable colorimetric visualization for the rapid and high selective detection of Hg^{2+}. *RSC Advances, 5*(124), 102542–102549.

Yi, Y. Z., Jiang, S. J., & Sahayam, A. C. (2012). Palladium nanoparticles as the modifier for the determination of Zn, As, Cd, Sb, Hg and Pb in biological samples by ultrasonic slurry sampling electrothermal vaporization inductively coupled plasma mass spectrometry. *Journal of Analytical Atomic Spectrometry, 27*(3), 426–431.

Zhang, G., Lin, W., Yang, W., et al. (2012). Logic gates for multiplexed analysis of Hg^{2+} and Ag^{+}. *Analyst, 137*(11), 2687–2691.

Zhou, N., Li, J., Chen, H., et al. (2013). A functional graphene oxide-ionic liquid composites–gold nanoparticle sensing platform for ultrasensitive electrochemical detection of Hg^{2+}. *Analyst, 138*(4), 1091–1097.

Zhu, M., Wang, Y., Deng, Y., et al. (2014). Ultrasensitive detection of mercury with a novel one-step signal amplified lateral flow strip based on gold nanoparticle-labeled ssDNA recognition and enhancement probes. *Biosensors and Bioelectronics, 61*, 14–20.